ilmedia

TECHNISCHE UNIVERSITÄT
ILMENAU

Zhang, Chen; Breitbarth, Andreas; Rosenberger, Maik; Notni, Gunther:

3D model based shading correction for the enhancement of multispectral colour measurement accuracy

Original published in: Journal of physics. Conference Series / Institute of Physics - Bristol : IOP Publ.. - 1065 (2018), art. 32008, 4 pp.

Original published: 2018-08-01

ISSN: 1742-6596

DOI: 10.1088/1742-6596/1065/3/032008

[*Visited:* 2020-06-09]

This work is licensed under a Creative Commons Attribution 3.0 Unported license. To view a copy of this license, visit https://creativecommons.org/licenses/by/3.0/

TU Ilmenau | Universitätsbibliothek | ilmedia, 2020
http://www.tu-ilmenau.de/ilmedia

IOP Conf. Series: Journal of Physics: Conf. Series **1065** (2018) 032008 doi:10.1088/1742-6596/1065/3/032008

3D model based shading correction for the enhancement of multispectral colour measurement accuracy

C Zhang[1,3], **A Breitbarth**[1], **M Rosenberger**[1], **and G Notni**[1,2]
[1] Ilmenau University of Technology, Group for Quality Assurance and Industrial Image Processing, Gustav-Kirchhoff-Platz 2, 98693 Ilmenau, Germany
[2] Fraunhofer Institute for Applied Optics and Precision Engineering, Albert-Einstein-Straße 7, 07745 Jena, Germany

E-mail: chen.zhang@tu-ilmenau.de

Abstract. Shading effects induced by illumination and local object surface orientation could strongly deteriorate the accuracy of colour imaging. Therefore, a shading correction is needed for high colour fidelity. In this work a 3D model based inverse rendering approach is proposed for a narrowband multispectral 3D colour imaging system with a calibrated extern broadband light source. The colourimetric evaluation with an X-Rite colour checker shows that the proposed method could ensure a mean colour difference value CIEDE2000 $\Delta E < 3$ for the viewing angle range -30° to 30°, while the maximal improvement factor concerning mean ΔE comes to 2.86.

1. Introduction and related work

Multispectral colour imaging technique could transcend the accuracy limitation of conventional RGB cameras and recognize minor colour differences. Hence it is widely used in food quality monitoring [1], biological imaging [2], medical skin imaging [3], cultural heritage [4] etc. A major challenge in colour reproduction is that the colour appearance of object surfaces can be strongly affected by illumination and viewing geometry. Therefore, reliable colour values could be captured only if colour measurements are performed with controlled lighting in regard to the CIE standard geometries [5], for instance the 45°-0° geometry (illumination at 45° and viewing at 0°) or 8° directional-hemispherical geometry using an integrating sphere. However, the realization of these standard geometries could be expensive for large imaging areas due to difficulties in the device manufacturing. Furthermore, at non-planar objects the local surface orientation is overall varying, so it is impossible to realize the CIE geometries for all object surface points, leading to shading effects that downgrade the colour accuracy.
For this problem, an inverse image rendering as shading correction could be performed to retrieve the pure material characteristics from raw image data. Considering that the shading effects are subordinate to the object form, the 3D object model should be the foundation of the shading correction. In [6] and [7] a colour value correction based on depth data and look-up-tables is realized for each image pixel. But in their work the local surface orientation, on which the incidence angle and thus the incident light density are dependent, is not utilized. Contrarily, the shading correction in [8] is based on local surface normal vectors estimated with high-resolution 3D models. But the influence of the distance between

[3] To whom any correspondence should be addressed.
This work has been sponsored by the German Federal Ministry of Education and Research in the program Zwanzig20 – Partnership for Innovation as part of the research alliance 3Dsensation (project number 03ZZ0462).

Content from this work may be used under the terms of the Creative Commons Attribution 3.0 licence. Any further distribution of this work must maintain attribution to the author(s) and the title of the work, journal citation and DOI.
Published under licence by IOP Publishing Ltd

illuminator and object is not involved in this inverse rendering, and the digital projector with a white LED that is used as illuminator cannot cover the entire visible spectral range 380-780 nm so that this method cannot be directly adopted for multispectral imaging systems.
In this article, a comprehensive 3D based shading correction method is presented for a multispectral colour imaging system. The proposed approach combines the usage of the depth data, surface normal, und a calibrated broadband light source. The colour accuracy at this system was evaluated with different object orientations.

2. Shading correction algorithm

Figure 1 illustrates the relation between light source, surface local geometry and observer camera. For the realistic modelling of reflector lamps the point light source model in [9] with non-isotropic angular emission is used, in which the angular radiant distribution around its light axis $\boldsymbol{l}_{\mathrm{axis}}$ is modelled using a polynomial function f_{ARD}. According to the photometric distance law, the incident light density L_{inc} at an object point P is dependent on the light axis $\boldsymbol{l}_{\mathrm{axis}}$, incident vector $\boldsymbol{l}$, and surface normal vector $\boldsymbol{n}$:

$$L_{\mathrm{inc}} \sim \frac{f_{\mathrm{ARD}}(\boldsymbol{l}, \boldsymbol{l}_{\mathrm{axis}}) \cdot \cos(\measuredangle(\boldsymbol{l}, \boldsymbol{n}))}{\|\boldsymbol{l}\|^2} = \frac{f_{\mathrm{ARD}}(\boldsymbol{l}, \boldsymbol{l}_{\mathrm{axis}}) \cdot \cos(\theta_{\mathrm{inc}})}{\|\boldsymbol{l}\|^2}. \tag{1}$$

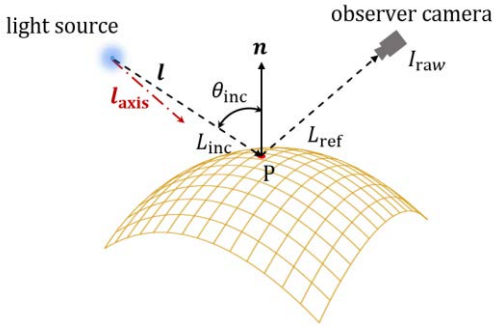

Figure 1. Photometric reflection model for Lambertian surface.

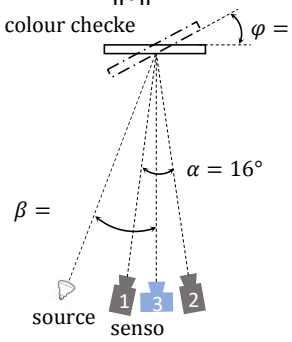

Figure 2. Schematic of the experimental setup. 1, 2: multispectral cameras. 3: pattern projector.

The reflection light density L_{ref} in the observation direction with respect to the surface normal is related to the bidirectional reflectance distribution function (BRDF) of the surface. In this work, the assumption of Lambertian reflection model is adopted. While this assumption may seem to be restrictive, it is the common approximation for the angular appearance of diffuse surfaces in a certain angle range. So, the shading correction is performed as inverse rendering relating to a pre-defined reference incidence angle θ_{r} and reference distance l_{r} between object and light source. In high-resolution 3D point clouds, local surface normal vectors can be efficiently and accurately computed with the principal component analysis (PCA) based method [10], enabling a robust estimation of light incidence angles θ_{inc}. Then, raw camera intensity values I_{raw} at each spectral channel can be normalized to I_{norm} with equation (2):

$$I_{\mathrm{norm}}(\theta_{\mathrm{inc}}, \boldsymbol{l}) = I_{\mathrm{raw}} \cdot \frac{\cos(\theta_{\mathrm{r}})}{\cos(\theta_{\mathrm{inc}})} \cdot \frac{\|\boldsymbol{l}\|^2}{{l_{\mathrm{r}}}^2} \cdot \frac{1}{f_{\mathrm{ARD}}(\boldsymbol{l}, \boldsymbol{l}_{\mathrm{axis}})}. \tag{2}$$

3. Experimental setup

Figure 2 illustrates the schematic of the experimental setup. It consists of a halogen lamp emitting at 30° as permanent illumination for the multispectral colour measurement and a sensor head composed of one digital pattern projector and two 8-bit multispectral filter wheel cameras [11] for the synchronous colour and 3D shape acquisition. This stereo camera system has 16° triangulation angle and 160 mm baseline. The spectral range 400-775 nm is split into 16 equidistant channels with 25 nm bandwidth that are set at both cameras, while the transversal interchannel pixel displacement is compensated using the radial-tangential model in [12]. Furthermore, both cameras have a shared channel at 550 nm, at which aperiodic sinusoidal fringe patterns [13] are projected for the accurate stereo matching. Thereby, the both partial multispectral images are pixel-wise registered into a full spectrum image, while the 3D object shape is

reconstructed via stereophotogrammetry. The rendered spectral values are then mapped to the CIE XYZ colour space under standard illuminant D65 using the linear matrix transform method in [14], whereas the matrix coefficients were estimated by a colour calibration with the X-Rite colour checker Passport. For light source calibration a diffuse and uniformly coloured plane target was utilized. This target was observed at 20 different poses with significant variation of position and orientation, at each of which the 3D model of the target and the 3D light intensity distribution on it were obtained. Then, the parameters in the light source model in [9] can be estimated from a non-linear data fitting, whereas the angular non-uniformity of light distribution is modelled with a quadratic function. The light source parameters are used for the shading correction both in the colour calibration and colour measurement.

4. Colourimetric evaluation results

The performance of the proposed shading correction approach was evaluated with experiments. Firstly, the spectral colour calibration was performed with the colour checker angle $\varphi = 0°$. Afterwards, the colour checker was captured in the angle range from -30° to 30° in step of 5°. For all 24 colour patches, the XYZ colour values are transformed to the L^*a^*b colour space, in which the ΔE colour difference values according to the CIEDE2000 standard [15] are calculated at these 13 angles. Figure 3(a) indicates the mean ΔE values calculated over all 13 viewing angles at these colour patches. A significant reduction of colour difference is achieved at 22 colour patches with shading correction. A minor increase of ΔE could be seen at the dark skin patch (bottom left) and black patch, probably due to the deteriorated 3D measurement accuracy in these areas with lower reflectance so that the normal estimation error grows.

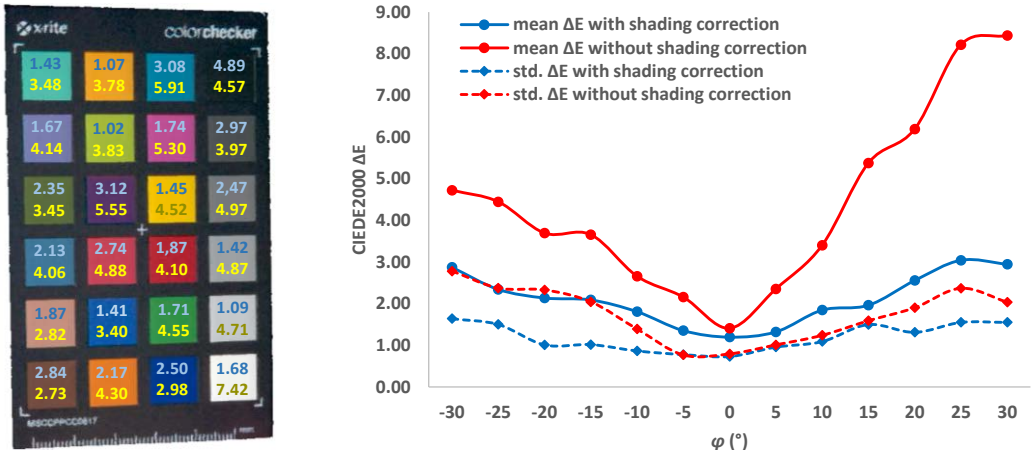

(a) (b)

Figure 3. Colourimetric evaluation results. (a**)**: mean ΔE over different viewing angles φ at 24 colour patches. Top/bottom: ΔE with/without shading correction. (b**)**: mean ΔE and standard deviation over all 24 colour patches at different colour checker orientations.

Figure 3(b) illustrates the mean ΔE and standard deviation over all 24 colour patches at different φ. First of all, it could be seen that the mean ΔE values and standard deviation calculated with raw spectral data rise strongly with the growth of angle φ. With the shading correction the mean ΔE could be reduced to smaller than 3 in the angle range -30° to 30°, while the standard deviation is lower than 1.65. At φ = 30°, an improvement factor of 2.86 concerning mean ΔE is reached. Nevertheless, there is still a minor ΔE increase with the angle growth. The reasons for it may be that the surface reflection does not perfectly match the Lambertian model at large viewing angles, and the errors in the light source calibration and surface normal estimation have an increased influence on the accuracy of inverse rendering in this case.

5. Summary and discussion

This work aims at the evaluation of the possibility of using inverse rendering based on 3D model and a calibrated light source for the improvement of multispectral colour imaging. The experimental results

show that the "acceptable tolerance" of $\Delta E = 3$ [16] could be ensured for a large viewing angle range at diffuse surfaces under the assumption of the Lambertian reflection model.
Considering the deviation of real object surfaces from the Lambertian model or for non-diffuse objects, multiple calibrated illuminators could be employed to sequentially illuminate the same object point from different directions for a pixel-wise model based BRDF estimation, so that their colour appearances at different viewing angles could be estimated.

6. References

[1] Kamruzzaman M, Makino Y and Oshita S 2016 Online monitoring of red meat color using hyperspectral imaging *Meat Science* ed D Hopkins vol. 116 pp 110-117
[2] Garcia J, Girard M, Kasumovic M, Petersen P, Wilksch P and Dyer A 2015 Differentiating Biological Colours with Few and Many Sensors: Spectral Reconstruction with RGB and Hyperspectral Cameras *Plos One 10 (5)* e0125817 p 31
[3] Kim S et al 2016 Smartphone-based multispectral imaging: system development and potential for mobile skin diagnosis *Biomedical Optics* Express vol. 7 issue 12 pp 5294-5307
[4] Rahaman G, Parkkinen J, Hauta-Kasari M and Amirshahi S 2017 Enhanced color visualization by spectral imaging: an application in cultural heritage *Proc. 2017 IEEE International Conference on Imaging, Vision & Pattern Recognition (icIVPR)* p 6
[5] Commission internationale de l'éclairage 2006 *Geometric Tolerances for Colour Measurements* (Vienna: CIE Central Bureau)
[6] Wu C-T and Allebach J 2015 Shading Correction of Camera Captured Document Image with Depth Map Information *Proc. SPIE* vol. 9395 no. 939505 p 7
[7] Eckhard T and Schnitzlein M 2016 Height adaptive shading correction for line-scan stereo imaging based multi-spectral reflectance measurements *Forum Bildverarbeitung 2016* ed M Heizmann, T Längle and F Puente Leon (Karlsruhe: KIT Scientific Publishing) pp 197-207
[8] Siepmann J, Heinze M, Kühmstedt P and Notni G 2009 Pixel synchronous measurement of object shape and colour *Proc. SPIE* vol. 7432 no. 74320Y-1 p 10
[9] Park J, Sinha S N, Matsushita Y, Tai Y-W and Kweon I S 2014 Calibrating a Non-isotropic Near Point Light Source Using a Plane *Proceedings of 2014 IEEE Conference on Computer Vision and Pattern Recognition (CVPR)* 35 pp 2267-2274
[10] Klasing K, Althoff D, Wollherr D and Buss M 2009 Comparison of surface normal estimation methods for range sensing applications *Proc. 2009 IEEE International Conference on Robotics and Automation (ICRA)* pp 3206-3211
[11] Rosenberger M, Preißler M, Fütterer R, Zhang C, Celestre R and Notni G 2016 Development and characterization of a high speed linear-moving-stage for multispectral measurements *Journal of Physics* vol. 772 p 6
[12] Zhang C, Celestre R, Rosenberger M and Notni G 2017 Exact correction of image distortion in a filter wheel multispectral camera with focus adjustment *Joint IMEKO TC1-TC7-TC13 Symposium: Measurement Science Challenges in Natural and Social Sciences* p 6
[13] Heist S, Kühmstedt P, Tünnermann A and Notni G 2015 Theoretical considerations on aperiodic sinusoidal fringes in comparison to phase-shifted sinusoidal fringes for high-speed three-dimensional shape measurement *App. Opt.* vol. 54 issue 35 pp 10541-1055
[14] Hardeberg J Y 2001 *Acquisition and Reproduction of Color Images: Colorimetric and Multispectral Approaches* (USA: Dissertation.com)
[15] Sharma G, Wu W and Dalal E N 2005 The CIEDE2000 Color-Difference Formula: Implementation Notes, Supplementary Test Data, and Mathematical Observations *Color Research & Application* vol. 30 no. 1 pp 21-30
[16] Stamm S 1981 An investigation of color tolerance *TAGA Proc.* pp 156-173